Revised manuscript submitted to: *The Journal of Supercritical Fluids*
(Ref. No.: SUPFLU-D-10-00098)

Hydrogenation of phenol with supported Rh catalysts in the presence of compressed CO_2: Its effects on reaction rate, product selectivity and catalyst life

Shin-ichiro Fujita,[†] Takuya Yamada,[†] Yoshinari Akiyama,[†] Haiyang Cheng,[‡] Fengyu Zhao,[‡] and Masahiko Arai[†]*

Division of Chemical Process Engineering, Graduate School of Engineering, Hokkaido University, Sapporo 060-8628, Japan

State Key Laboratory of Electroanalytical Chemistry, Changchun Institute of Applied Chemistry, Chinese Academy of Sciences, Changchun 130022, P. R. China

* Corresponding author. Tel & Fax: +81-11-706-6594, E-mail: marai@eng.hokudai.ac.jp

[†] Hokkaido University

[‡] Changchun Institute of Applied Chemistry

ABSTRACT

Hydrogenation of phenol to cyclohexanone and cyclohexanol in/under compressed CO_2 was examined using commercial Rh/C and Rh/Al_2O_3 catalysts to investigate the effects of CO_2 pressurization on the total conversion and the product selectivity. Although the total rate of phenol hydrogenation with Rh/C was lowered by the presence of CO_2, the selectivity to cyclohexanone was improved at high conversion levels > 70%. On the other hand, the activity of Rh/Al_2O_3 was completely lost in an early stage of reaction. The features of these multiphase catalytic hydrogenation reactions using compressed CO_2 were studied in detail by phase behavior and solubility measurements, *in situ* high pressure FTIR for molecular interactions of CO_2 with reacting species and formation/adsorption of CO on the catalysts, and simulation of reaction kinetics using a simple model. The CO_2 pressurization was shown to suppress the hydrogenation of cyclohexanone to cyclohexanol, improving the selectivity to cyclohexanone. The formation and adsorption of CO were observed for the two catalysts at high CO_2 pressures in the presence of H_2, which was one of important factors retarding the rate of hydrogenation in the presence of CO_2. It was further indicated that the adsorption of CO on Rh/Al_2O_3 was strong and caused the complete loss of its activity.

Keywords: Rhodium; Hydrogenation; Supercritical CO_2; Cyclohexanone; Cyclohexanol

1. Introduction

Catalytic hydrogenation of phenol is industrially important for the synthesis of cyclohexanone and cyclohexanol as the intermediate for the manufacture of nylon-6 and -66.[1] Generally, the hydrogenation of phenol is carried out in the vapor phase over supported Pd catalysts [1-12]. In the cases of vapor phase hydrogenation, high temperatures are needed, which usually cause catalyst deactivation by coking during the reaction. In a few studies, liquid phase hydrogenation of phenol was carried out with Pd catalysts [13-16]. However, high reaction temperatures or long reaction time were still required to obtain high phenol conversions.

Supercritical carbon dioxide ($scCO_2$) has been gaining considerable interests as an ecologically benign new reaction medium [17-21]. Rode et al. showed that a charcoal-supported rhodium (Rh/C) catalyst was highly active for the ring hydrogenation of phenol and cresols in $scCO_2$, and high conversions of phenol were achieved over Rh/C under such conditions as 328 K, 10 MPa H_2, and 12 MPa CO_2 [22]. Carbon supported Pd, Ru and Pt catalysts were much less active than Rh/C. Our group has also reported that a Rh catalyst supported on carbon nanofiber is active for the phenol hydrogenation in $scCO_2$ at a low temperature of 323 K and at a lower hydrogen pressure of 4 MPa [23]. Recently, Chatterjee et al. have screened several supported catalysts using different noble metals and supports and found that Pd on Al-MCM-41 is effective to the hydrogenation of phenol to cyclohexanone in dense phase CO_2 (12 MPa) [24]. Very recently Liu et al. indicated an interesting synergistic effect of supported Pd particles and solid Lewis acid, with which the hydrogenation of phenol to cyclohexanone was achieved in almost 100% selectivity under mild conditions [25].

Those results indicate the interesting features of phenol hydrogenation using supported metal catalysts and dense phase CO_2. However, the details of these complicated multiphase reactions are still unknown. The reaction rate and the product distribution should depend on several factors [26]. Our group has reported that interactions of carbonyl group with CO_2 molecules can cause the enhancement in the reactivity and/or the change in the reaction selectivity [27-30]. Conversion and selectivity of hydrogenation of α, β-unsaturated aldehydes (cinnamaldehyde and citral) to unsaturated alcohols were significantly enhanced by the presence of pressurized CO_2 [27-30]. Enhancement in the product yield by pressurized CO_2 was also observed for Heck reactions that did not involve gaseous reactants like hydrogen [30]. The molecular interactions between carbonyl group and CO_2 were shown to depend significantly on the structure of the carbonyl compounds [31]. It is known that an organic liquid phase expands when it is pressurized by CO_2 and the extent of volume expansion may change with the kind of organic liquid and the CO_2 pressure [32-36]. These CO_2-dissolved expanded liquid phases are demonstrated to be interesting reaction media for reactions including gaseous reactants like O_2, H_2, and CO. Moreover, it is reported that CO may be formed in hydrogenation reactions with supported noble metal catalysts in $scCO_2$ and this has negative impacts on the catalytic activity and, subsequently, the reaction rate and selectivity [37-42].

The present work has been undertaken to investigate in detail the hydrogenation of phenol in/under pressurized CO_2 using commercial Rh/C and Rh/Al_2O_3 catalysts. In addition to the reaction runs, the authors have made the simulation of reaction kinetics and examined the phase behavior of reaction mixture and the solubility of reacting species (phenol and cyclohexanone) in pressurized CO_2. Furthermore, *in situ* high-pressure transmittance FTIR measurements have been made to study the molecular interactions of the reacting species with CO_2 and the formation and adsorption of CO on the catalysts at high pressures. *In situ* high-pressure measurement of the formation of CO from pressurized CO_2 and H_2 over supported metal catalysts was studied only by Baiker et al., who used attenuated total reflection infrared (ATR-IR) spectroscopy [37,38,40]. In the present work, those reaction, characterization, and simulation results have been used to clarify the features of the hydrogenation of phenol, the influence of CO_2 pressurization on the reaction rate and the product selectivity, and significant factors responsible for the effects of CO_2 pressurization on this hydrogenation.

2. Experimental

2.1. Catalyst and characterization Commercially available 5 wt.-% Rh/C and 5 wt.-% Rh/Al_2O_3 catalysts (Wako) were used without further treatments. The degree of metal dispersion of these catalysts was determined by hydrogen adsorption. After the catalyst sample was reduced with flowing hydrogen at 373 K for 1 h and treated with flowing helium at 473 K for 30 min, hydrogen was adsorbed on the sample at 323 K. The dispersion of Rh was calculated from the amount of hydrogen adsorbed on the assumption of H/Rh = 1. The dispersion values thus determined were 44.3% and 30.9% for Rh/C and Rh/Al_2O_3, respectively. The surface properties of these supported Rh particles were examined by X-ray photoelectron spectroscopy (Shimadzu ESCA3200). Catalyst samples were dispersed on carbon tape and X-ray photoelectron spectra were collected without any pretreatment. Correction of the spectra was made on the basis of the Au $4f_{7/2}$ line at 83.8 eV of gold wire that was placed on the edge of the carbon tape together with the catalyst sample.

2.2. Hydrogenation reaction The hydrogenation reaction runs were carried out in a 50 cm^3 stainless steel autoclave. In a typical run, 20 mg of Rh/C and 10.6 mmol of phenol were charged into the reactor and the reactor was flushed with H_2 three times to remove the air. This purge of the reactor had no significant impact on the amount of phenol at the start of reaction. After the reactor was heated up to 323 K, H_2 (4 MPa) was introduced, and then compressed liquid CO_2 was fed into the reactor with a high-pressure liquid pump attached with a cooler (JASCO SCF-GET). The reaction runs were conducted while stirring with a magnetic stirrer. At the end of the reaction, the autoclave was cooled to room temperature and then depressurized carefully by a backpressure regulator (JASCO SCF-bpg). The composition of reaction mixture was

analyzed by a gas chromatograph (GL Science GC-900B) using a capillary column (Zebron ZB-WAX) and a flame ionization detector. In several runs, the phenol conversion was controlled to be below 10% by decreasing the catalyst amount and shortening the reaction time to measure the initial rate of reaction. For comparison, hydrogenation of cyclohexanone was also conducted in similar manners. The total conversion of phenol was determined by 1 - (the final amount of phenol unreacted / the initial amount of phenol loaded). The yield of cyclohexanone (or cyclohexanol) was calculated by the amount of cyclohexanone (or cyclohexanol) formed / the initial amount of phenol loaded. The selectivity to cyclohexanone was determined by the amount of cyclohexanone formed / the total amount of cyclohexanone and cyclohexanol formed. No other products were observed in our reaction runs. The conversion and selectivity values could be determined with $< \pm 5\%$ relative errors under the conditions used.

In some reaction runs using CO_2, gases in the reactor were collected and analyzed by a gas chromatograph (Hitachi G3000) equipped with a MS-5A column, a methanizer and a flame ionization detector, to investigate the formation of gaseous CO.

2.3. Solubility in pressurized CO_2 The solubility of phenol in CO_2 was measured with a 10 cm^3 high-pressure view cell equipped with two sapphire windows. The cell was charged with a certain amount of substrate, flushed with 0.2-0.3 MPa CO_2 twice, and heated up to 323 K (reaction temperature) by the circulation of preheated oil around it (JULABO F25-HP). Then, liquid CO_2 was introduced into the cell and stirring was started. When the pressure reached to the desired value, the stirring was continued further for 5 min and stopped; then, the state of the mixture including the substrate and CO_2 was visually inspected. This examination was made at intervals of 0.2-0.5 MPa to determine the pressure at which the substrate was completely dissolved into CO_2, forming a single phase. These measurements were also made for the products of cyclohexanone and cyclohexanol to determine the solubility of them. Changes in the volume of the liquid phases by pressurization with CO_2 were also investigated with an 85 cm^3 high-pressure view cell in procedures similar to those for the solubility measurement.

2.4. *In situ* FTIR in pressurized CO_2 The FTIR spectra of phenol and cyclohexanone in pressurized CO_2 medium were measured *in situ* with an FT-IR spectrometer (JASCO FTIR-620) equipped with a 1.5 cm^3 high pressure cell with an optical path length of 4 mm. The FTIR measurements were made at 323 K and at CO_2 pressures up to 20 MPa. A small volume (about 0.01 cm^3) of a sample carbonyl compound was introduced into the cell and it was purged with CO_2 three times. The cell was heated up to a temperature of 323 K by the circulation of preheated oil around it. Then, the pressure was increased slowly by introduction of liquid CO_2 by the high-pressure liquid pump while stirring by a Teflon coated magnetic stirrer. When the pressure reached a certain value, the stirring was further continued for 2 min and stopped. The FTIR spectra were measured with a triglycine sulfate (TGS) detector at a wavenumber resolution of 2 cm^{-1} by using the absorption spectrum of pure CO_2 at the same pressure as background. For

comparison, the gas and liquid phase spectra of phenol and cyclohexanone were also collected. The gas phase spectra were measured with the above-mentioned cell at 323 K in ambient CO_2 atmosphere. The liquid spectra were measured at ambient temperature for a thin liquid film jammed by KBr crystal plates.

For the purpose of obtaining direct evidence for the formation of adsorbed CO in the mixture of compressed CO_2 and H_2, the authors made a stainless steel cell with ZnSe windows for *in situ* transmittance FTIR measurements at high pressures. The cell temperature was controlled by using four rod heaters put in the wall of the cell. A mixture of Rh/C (10 mg) and a silica gel (20 mg) or Rh/Al_2O_3 alone (30 mg) was pelletized and put into the cell. The cell was introduced with H_2 up to 4 MPa and the sample was reduced at 323 K for 1 h in the closed cell. After passing H_2 through the cell for a while, H_2 was again introduced up to 4 MPa. Then, CO_2 was introduced and FTIR measurements were made at different CO_2 pressures. The FTIR spectra were collected at 323 K using the spectra obtained at the same CO_2 pressures in the absence of catalyst sample as backgrounds.

3. Results

Under the conditions employed in the present study, oxygen-containing cyclohexanone and cyclohexanol were observed to form but no hydrocarbon products such as benzene, cyclohexane and cyclohexene were detected. The rate of phenol conversion and the product selectivity were found to depend on CO_2 pressure and the catalysts used.

3.1. Rh/C catalyst Fig. 1 represents the variations of the phenol conversion and the product yields with reaction time obtained using Rh/C in the absence and presence of 16 MPa CO_2. Fig. 1a indicates that the yield of cyclohexanone increased with time and then decreases through a maximum at around 30 min, while that of cyclohexanol increased monotonically in the absence of CO_2. Similar trends were also observed in the presence of CO_2 at 16 MPa (Fig. 1b) and lower pressures. In Fig. 2, the selectivity to cyclohexanone is plotted against the phenol conversion. At extrapolated zero phenol conversion, the selectivity to cyclohexanone was around 60% irrespective of CO_2 pressures used. When the conversion increased up to 70%, the selectivity to cyclohexanone gradually decreased. The presence of pressurized CO_2 had no effect on the product selectivity at conversions between 0 and 70%. At larger conversions, however, the selectivity to cyclohexanone decreased rapidly with the conversion in the absence of CO_2, whereas the selectivity also decreased in the presence of CO_2 but gradually similar to the change at lower conversions. The selectivity to cyclohexanone at 100% conversion was < 10% in the absence of CO_2 but about 40% in the presence of CO_2 at 4 - 16 MPa. As a result, the selectivity to cyclohexanone obtained in the presence of CO_2 was always higher irrespective of CO_2 pressures than that in the absence of CO_2.

Figure 1, Figure 2

The apparent initial rates of phenol hydrogenation, moles of phenol consumed per unit time per unit weight of catalyst, were measured in the presence of CO_2 at various pressures to investigate the influence of CO_2 on the reaction. Fig. 3a gives the initial rate against the CO_2 pressure. In the presence of CO_2 at pressures between 1 and 13 MPa, the rate was smaller by a factor of 1/3 than that in the absence of CO_2. When the pressure was raised to 14 MPa, the initial rate increased, but it did not change so much at higher pressures. The rate obtained in the presence of CO_2 was smaller than that in the absence of CO_2. Thus, pressurized CO_2 had negative effect on the rate of hydrogenation of phenol. In addition, the apparent initial rate of hydrogenation of cyclohexanone, instead of phenol, was measured at different CO_2 pressures (Fig. 3b). Similar rates appeared in the presence of CO_2, which were about 1/3 of the one obtained in the absence of CO_2. Similar to phenol, the CO_2 pressurization had negative effect on the rate of hydrogenation of cyclohexanone. In contrast to phenol in which the rate increased with CO_2 pressure at 14 MPa or above, for the hydrogenation of cyclohexanone in the presence of CO_2, the rates were similar irrespective of CO_2 pressures (4 - 20 MPa).

Figure 3

3.2. Rh/Al_2O_3 catalyst Similar reaction runs were also carried out with Rh/Al_2O_3 catalyst for comparison. Fig. 4 represents the variations of the phenol conversion and the product yields with time in the absence of CO_2. The yield of cyclohexanone showed a maximum at around 30 min, whereas that of cyclohexanol increased monotonically with time. Thus, the results obtained in the absence of CO_2 with Rh/Al_2O_3 were very similar to those obtained with Rh/C (Fig. 1). When the reaction was conducted in the presence of CO_2, different results were obtained. Fig. 5 gives the results obtained at CO_2 pressures of 8 and 14 MPa, indicating that the hydrogenation reaction of phenol stopped in an early stage of reaction. That is, the activity of Rh/Al_2O_3 was rapidly and completely lost during the reaction. Note that the reaction stopped in about 30 min at 8 MPa but in a shorter time of 5 min at a higher CO_2 pressure of 14 MPa.

Figure 4, Figure 5

Fig. 6 represents the influence of CO_2 on the relationship between the phenol conversion and the product selectivity over Rh/Al_2O_3. It was not possible to get high conversion in the presence of CO_2 because of the rapid catalyst deactivation as mentioned above. Similar to the results obtained over Rh/C, the presence of CO_2 had no effect on the selectivity at low and medium conversions. Comparison of Figs. 2 and 6 shows that, in the absence of CO_2, the selectivity to cyclohexanone over Rh/Al_2O_3 was about 15% higher than that over Rh/C in the

whole range of phenol conversion.

Figure 6

3.3. Solubility in pressurized CO_2 The solubility of reacting species in CO_2 gas phase is one of important factors determining the outcome of multiphase reactions using pressurized CO_2. Fig. 7 shows the solubility of phenol, cyclohexanone, and cyclohexanol in CO_2 in the presence of 4 MPa H_2 at a reaction temperature of 323 K. The solubility was cyclohexanone >> cyclohexanol > phenol. For the reaction runs, 10.6 mmol of phenol was charged in the reactor volume of 50 cm^3 and the initial concentration of phenol was 0.21 mmol cm^{-3}. So, the reaction mixture should change from solid–liquid–gas three-phase state to solid–gas two-phase state at a CO_2 pressure around 14 MPa. It should be noted that this pressure accorded with the pressure at which the initial rate of phenol hydrogenation was observed to increase (Fig. 3a).

Figure 7

Furthermore, the volume expansion of organic liquids on CO_2 pressurization was measured for phenol and cyclohexanone with similar liquid/reactor volume ratio as used in the reaction runs. It was found that the latter expanded significantly by pressurization with CO_2, while such expansion was not observed for the former (Fig. 8). The extent of volume expansion of liquid cyclohexanone is plotted against CO_2 pressure in Fig. 9. The volume increased slightly with the pressure up to 6 MPa and significantly at higher pressures. The expansion is caused from the dissolution of CO_2 molecules into the liquid phase [26,32-36]. CO_2-expanded liquid phase has recently been gaining considerable attention, because it will facilitate the dissolution of other coexisting gases of H_2, O_2, CO, and so on and may accelerate the reactions involved with these gaseous reactants although CO_2 is not a reactant but rather a diluent [26-28,32-36].

Figure 8, Figure 9

3.4. In situ high pressure FTIR Interactions of CO_2 with reacting organic compounds were examined by *in situ* high pressure FTIR spectroscopy at 323 K. The FTIR spectra of phenol were measured in pressurized CO_2 at different pressures and similar spectra were obtained. It is unlikely, therefore, that the reactivity of phenol is modified by CO_2. Fig. 10 shows FTIR spectra in the region of carbonyl absorption for cyclohexanone in liquid and gas states and in CO_2. Liquid cyclohexanone exhibited a broad absorption band assigned to ν(C=O) at 1710 cm^{-1}. This band of gaseous cyclohexanone was shifted to a larger wavenumber by 30 cm^{-1} compared with the liquid state. For the spectra measured in CO_2, the ν(C=O) band was located at a position between those of liquid and gaseous cyclohexanone and red-shifted with CO_2 pressure. This red-shift would result from Lewis acid - base type interactions between CO_2 and its carbonyl

group, as previously discussed [28,31]. Other absorption bands due to C-H and C-C bonds were not observed to be shifted with CO_2 pressure.

Figure 10

Furthermore, *in situ* high-pressure transmittance FTIR was used to examine the formation of CO from compressed CO_2 and H_2. Fig. 11 shows the spectra for Rh/Al_2O_3 obtained at different times after the introduction of CO_2 up to 4 MPa and 16 MPa. At 4 MPa CO_2, absorption bands appeared at 2069, 2020, and 1844 cm^{-1} and the one also seemed to exist at 1970 cm^{-1}, which were assignable to various types of CO adsorbed on Rh as summarized in Table 1 according to the literature [42-44]. The strength of a weak absorption band at 2069 cm^{-1} seemed to increase with time but marginally. Similar absorption bands were observed but stronger at a higher CO_2 pressure of 16 MPa. These results give direct evidence that CO is formed from the mixture of compressed CO_2 and H_2 in the presence of Rh/Al_2O_3 catalyst and CO is adsorbed on the surface of supported Rh particles in different modes. It is further indicated that the type of adsorbed CO species little depends on CO_2 pressure but the amount of CO adsorbed seems to be larger at 16 MPa than that at 4 MPa. In addition to those absorption bands due to the various types of adsorbed CO species, broad absorption bands were also observed at 1700 – 1200 cm^{-1}, which may indicate the presence of formate species [42,45-49] and/or other carbonyl groups [49] such as -COOH and -COO- on the support.

Figure 11, Table 1

The same FTIR measurements were also conducted with Rh/C sample. The formation and adsorption of CO on Rh in the mixture of compressed CO_2 and H_2 were also evidenced. The FTIR spectra collected are presented in Fig. 12. At 4 MPa CO_2, an absorption band was seen at 2069 cm^{-1} with a shoulder at smaller wavenumbers but no absorption was detected at 2020 - 1850 cm^{-1}, in contrast to the abovementioned spectra for Rh/Al_2O_3. The spectra at 16 MPa were very similar to those at 4 MPa but the amount of adsorbed CO was larger at 16 MPa. The Rh/C catalyst did not indicate the absorption bands due to formate at 1700 – 1200 cm^{-1} at both CO_2 pressures. The difference in the surface properties such as acidity would explain the formation of the formate on Rh/Al_2O_3 but not on Rh/C. Acidic surface of the support Al_2O_3 may interact with basic CO_2 molecules and facilitate the formation of the formate species [45-49]. The comparison of the spectra of Fig. 11 and Fig. 12 shows that the types of adsorbed CO species are different between Rh/C and Rh/Al_2O_3 catalysts. That is, the majority is of linear type for the former while the other types (dicarbonyl, bridged, triply bridged) also exist for the latter. This difference may be related to difference in the stability (strength) of adsorbed CO species, as described in the following.

Figure 12

In addition, FTIR spectra were measured after the IR cell was depressurized to ambient pressure following the FTIR measurements at 16 MPa CO_2 and at 323 K. Fig. 13 compares the spectra collected at 16 MPa and at ambient pressure. It is interesting to note that no absorption was observed in the range of wavenumber due to the adsorbed CO species for Rh/C. For Rh/Al_2O_3, the absorption band due to the linear type of adsorbed CO at 2073 cm^{-1} also disappeared on depressurization; however, the absorption bands assignable to the adsorbed CO of the other types and formate species still remained at ambient pressure. These absorption bands remained unchanged after the IR cell was purged with 0.1 MPa H_2. That is, for Rh/C, the CO species can be adsorbed on its surface in the presence of compressed CO_2 but not in the absence of compressed CO_2. For Rh/Al_2O_3, in contrast, the CO species can be adsorbed even at ambient pressure but only those of the types other than the linear one. Note that the formation and adsorption of CO under high pressure conditions cannot be denied even though no adsorption is detected under ambient conditions (for Rh/C in the present case).

Figure 13

4. Discussion

4.1. Reaction pathways of phenol hydrogenation As shown in Fig. 1, the yield of cyclohexanone was maximal in the course of the reaction with Rh/C, whereas that of cyclohexanol increased monotonously with time and it was likely to form at the expense of cyclohexanone in the latter stage of reaction. Similar results were obtained with Rh/Al_2O_3 in the absence of CO_2 (Fig. 4). These results strongly suggest that cyclohexanol is formed through the hydrogenation of cyclohexanone. If cyclohexanol was always produced by the hydrogenation of cyclohexanone, the selectivity to cyclohexanone would be 100% at zero conversion; however, this is not the case, as shown in Figs. 2 and 6. It is assumed, therefore, that cyclohexanone and cyclohexanol are produced through parallel pathways at low conversion levels. On the basis of these results, it can be concluded that the phenol hydrogenation proceeds through the pathways illustrated in Scheme 1: phenol is sequentially hydrogenated through cyclohexanone to cyclohexanol (paths i and iii) and directly to cyclohexanol (path ii). In contrast to the present results, almost 100% selectivity to cyclohexanone was obtained with supported Pd catalysts in both the gas–phase [1-12] and liquid–phase [13-16,25] hydrogenation reactions. The direct formation of cyclohexanol from phenol (path ii) is unlikely to occur with these Pd catalysts. The difference between the Rh and Pd catalysts is interesting but difficult to explain at present.

Scheme 1

4.2. Simulation of reaction kinetics The three pathways of Scheme 1 are assumed to be first order reactions with respect to the quantities of phenol and cyclohexanone. The apparent total rate of phenol consumption, r_0, moles of phenol consumed per unit time per unit weight of catalyst, is given as:

$$-r_0 = (k_1 + k_2)Q_0 \quad (1)$$

the rates of cyclohexanone and cyclohexanol formations, r_1 and r_2, are respectively given as

$$r_1 = k_1Q_0 - k_3Q_1 \quad (2)$$

$$r_2 = k_2Q_0 + k_3Q_1 \quad (3)$$

where k_1, k_2 and k_3 are rate constants of the corresponding pathways in Scheme 1 and Q_0, Q_1 and Q_2 are the quantities of phenol, cyclohexanone and cyclohexanol in the reactor, respectively. Using these simplified reaction rates, we calculated the variations of phenol conversion (X_0), cyclohexanone yield (Y_1), and cyclohexanol yield (Y_2) with reaction time by the following equations:

$$X_0 = 1 - \exp[-(k_1 + k_2)wt] \quad (4)$$

$$Y_1 = k_1\{\exp[-(k_1 + k_2)wt] - \exp(-k_3wt)\}/(k_3 - k_1 - k_2) \quad (5)$$

$$Y_2 = X_0 - Y_1 \quad (6)$$

where w is the amount of catalyst used and t is time. These kinetic equations were used to simulate the results of hydrogenation reactions of phenol obtained under different conditions. Fig. 14 shows the simulation results for the reactions with Rh/C at CO_2 pressures of 0, 4, and 16 MPa using the values of the rate constants listed in Table 2. The variations of the total conversion and the product yields with reaction time can be well fitted by this simulation, except for the results at high conversion levels at a CO_2 pressure of 4 MPa.

Figure 14, Table 2

In a similar manner, the simulation was made for the results with Rh/Al_2O_3 in the absence of CO_2 (Fig. 15). The values of the rate constants used for this simulation are also given in Table 2. Also for Rh/Al_2O_3, the simulation can well fit the experimental reaction results obtained. The difference of the rate constants between Rh/C and Rh/Al_2O_3 will be discussed later.

Figure 15

Next, the relationship between the total conversion and the product selectivity was calculated using the above-mentioned kinetic equations and the rate constants determined (Table 2). Fig. 16 shows that the experimental results are well simulated for the hydrogenation reactions of phenol with Rh/C and Rh/Al_2O_3. The present kinetics model can explain the gradual decrease of the selectivity to cyclohexanone with the conversion up to 70% and the marked difference in the selectivity at higher conversion levels between the reactions with Rh/C in the presence and

absence of CO_2. For Rh/C, all the rate constants are smaller in the presence of pressurized CO_2. However, the extent of the decrease of k_3 by the presence of CO_2 is the largest among the rate constants. Thus, the CO_2 pressurization has stronger impact on the reaction pathway iii than on the ones i and ii (Scheme 1). In other words, the hydrogenation of cyclohexanone to cyclohexanol can be suppressed in the presence of pressurized CO_2 more significantly than the hydrogenations of phenol to cyclohexanone and to cyclohexanol. Probably, this would be caused by the difference in the required adsorption mode between the phenol and cyclohexanone hydrogenation reactions. For the former reaction, the adsorption of aromatic ring on Rh surface is required, while the adsorption of C=O group is required for the latter reaction.

Figure 16

4.3. Influence of pressurized CO_2 on phenol hydrogenation The initial rates of phenol and cyclohexanone hydrogenation reactions were measured with Rh/C in the presence of 8 MPa N_2 instead of CO_2. The rate of phenol hydrogenation obtained was 62.0 mmol min^{-1} g^{-1} and the selectivity to cyclohexanone was 45.3% at a phenol conversion of 58.6% and decreased to 1.4% at 98.6% conversion. In addition, the hydrogenation of cyclohexanone was conducted under the same conditions and the initial rate was 61.7 mmol min^{-1} g^{-1}. Comparison of these data with those of Fig. 2 shows that the presence of the compressed inert N_2 gas had no effect on the hydrogenation reactions of these substrates. Thus, it can be said that the effects of pressurized CO_2 resulted from its physicochemical nature but not simply its static pressure.

The initial rate of phenol hydrogenation with Rh/C was retarded by CO_2 (Fig. 3a) and the reaction with Rh/Al_2O_3 in the presence of CO_2 stopped in a short period of reaction time (Fig. 5). The FTIR results showed that there was no interaction of phenol with CO_2 and its reactivity was not changed by CO_2. A few possible factors may be related to the retardation effect of CO_2 observed. The first one is the formation of CO species adsorbed over Rh surface. It was confirmed by *in situ* high-pressure FTIR (Fig. 11) that the adsorbed CO was produced from CO_2-H_2, although no gaseous CO was detected in the gas phase after the hydrogenation runs in the presence of CO_2. Several research groups reported, by FTIR (not *in situ*), the formation of adsorbed CO from CO_2-H_2 mixtures via reverse water gas shift reaction over Pt [37-40], Rh [40], Ru [40,41], and Pd [40,41] catalysts even at such a low temperatures as 323 K. Some authors have also shown that adsorbed CO suppresses hydrogenation of ethyl pyruvate over Pt/Al_2O_3 [38] and dechlorination of chloroaniline over Pt/C [39]. Hence, the formation and adsorption of CO should retard the phenol hydrogenation by blocking Rh active site. In the case of Rh/Al_2O_3, the CO adsorption is so strong that its activity is completely lost during the reaction in the presence of CO_2 (Fig. 5). CO is formed along with water through the reverse water gas shift reaction. The amount of water formed was not measured in the present work but it should be small since the amount of CO in the gas phase was unable to be measured by GC. It is supposed that the water molecules formed are likely to be adsorbed on the supports rather than the Rh

particles and so the water would be less significant for the hydrogenation of phenol that occurs on the surface of supported Rh particles.

Another possible factor is the competitive adsorption of CO_2 and the substrate phenol on the catalyst surface. The adsorption of CO_2 could make the adsorption of phenol difficult, resulting in the retardation of its hydrogenation. However, this is implausible, because some reaction time was needed for the reaction with Rh/Al_2O_3 to completely stop and the time for the complete deactivation depended on the CO_2 pressure (Fig. 5). If the competitive adsorption of CO_2 and phenol is important, the catalyst deactivation should occur shortly after the start of reaction at any CO_2 pressures since the adsorption usually reaches its equilibrium rapidly irrespective of the pressure. It was previously reported that the amount of adsorbed CO produced from CO_2 gradually increased with time [37,40]. This can explain the induction period for the complete deactivation of Rh/Al_2O_3 catalyst. It can be noted again that the formation of adsorbed CO is one of important reasons for the retardation effect of CO_2 in phenol hydrogenation in the presence of CO_2.

A different factor is the simple dilution effect that the dissolution of CO_2 occurs into the liquid substrate phase under pressurized conditions and this would promote the dissolution of H_2 but, at the same time, decrease the concentration of the substrate in the reaction medium and make it more difficult for the substrate to contact with the catalyst. This negative, dilution effect should also be important for the retardation effect of CO_2 on the hydrogenation reaction of phenol. When the pressure is raised, phenol is likely to dissolve in the CO_2 gas phase more significantly and the hydrogenation reactions should take place in both liquid and gas phases. Although the rate constants k_1 and k_2 are not different between in the liquid phase (of G-L-S) and in the gas phase (of G-S) reactions, the concentration of the substrates is more diluted in the CO_2 gas phase. This negative effect should be significant at high CO_2 pressures above the pressure at which the reaction mixture changes from the G-L-S state to the G-S state. If this negative effect could be overcome by positive effects of complete miscibility of H_2 and fast mass transfer in the G-S mixture, the rate of reaction would be improved on the change of phase behavior. This could be the case for the increase in the rate of phenol hydrogenation at about 14 MPa as shown in Fig. 3b.

The initial rate of cyclohexanone hydrogenation was also retarded by the presence of CO_2 (Fig. 3b), similar to phenol, and this retardation would also be caused by the formation of adsorbed CO. The FTIR results with cyclohexanone showed the red shift of its ν(C=O) absorption band with CO_2 pressure, suggesting that the reactivity of its carbonyl group is enhanced with CO_2 pressure (Fig. 10). However, this positive effect of CO_2 should be overcome by the negative effect of the adsorbed CO produced from CO_2 and H_2. In contrast to phenol, the volume expansion of cyclohexanone on CO_2 pressurization was more remarkable (Fig. 9), implying that a larger quantity of CO_2 was dissolved into the cyclohexanone. The phase change of the G-L-S to the G-S occurred at a lower pressure of about 11 MPa due to the larger solubility of cyclohexanone in CO_2 (Fig. 7). As above-mentioned, the volume expansion gives a positive

effect of facilitating the dissolution of H_2 but a negative effect of the dilution of the reacting species and the phase change also has positive (complete miscibility of H_2) and negative (fast mass transfer and/or unknown factors) effects. Those positive and negative effects should depend on the CO_2 pressure. The superiority and inferiority of those pressure-dependent effects could result in similar reaction rates in the presence of CO_2 at 4 - 20 MPa irrespective of the pressure; the reaction is likely to occur in the liquid phase, in the liquid and gas phases, and in the gas phase at low, phase transition, and high pressures, respectively.

4.4. Comparison of Rh/C and Rh/Al_2O_3 The apparent initial rate of phenol consumption, $(k_1 + k_2)Q_0$, and the cyclohexanone selectivity at a conversion of zero, $k_1/(k_1 + k_2)$, were estimated from the rate constants listed in Table 2. Table 3 compares the total activity and the cyclohexanone selectivity between Rh/C and Rh/Al_2O_3 catalysts in the absence of CO_2. The latter was more active than the former and the turnover frequency (TOF, molecules of phenol consumed per an exposed Rh atom per unit time) of Rh/Al_2O_3 was about twice that of Rh/C. This may result from difference in the acid-base properties of the supports and/or that in the electronic properties of supported Rh crystallites. The cyclohexanone selectivity over Rh/Al_2O_3 was 15% higher than that over Rh/C. According to Scheme 1, the selectivity to cyclohexanone at low phenol conversions can be determined by the relative rates of pathways i and ii (k_1/k_2). As shown in Table 3, the value of k_1/k_2 over Rh/Al_2O_3 is above twice that over Rh/C. This may result from stronger acidity of Al_2O_3 support compared with active carbon. Liu et al. point out the significance of Lewis acidity of support materials in determining the high selectivity to the formation of cyclohexanone, which is prevented from being hydrogenated to cyclohexanol by interactions between the acid sites and the cyclohexanone [25].

Table 3

The effects of CO_2 pressurization were greatly different between Rh/C and Rh/Al_2O_3 catalysts. The activity of the former was somewhat lowered by the presence of CO_2 (Fig. 3a), while the latter lost its activity completely within a short period of reaction time in the presence of CO_2 (Fig. 5). One of significant factors is the difference in the nature of adsorbed CO between Rh/C and Rh/Al_2O_3. In contrast to the former, the adsorption of CO on the latter is so strong and it still remains adsorbed at ambient pressure (Fig. 13), causing the stronger inhibition effect of CO on Rh/Al_2O_3. This might depend on difference in the electronic properties of Rh particles dispersed on C and Al_2O_3 supports, which was indicated by XPS measurements (Fig. 17). It was indicated that the binding energy of either Rh $3d_{5/2}$ or Rh $3d_{3/2}$ was larger for Rh/Al_2O_3 than for Rh/C. The surface of Rh particles on Al_2O_3 was likely to be beneficial for CO to be adsorbed with 5σ electron to the exposed Rh atoms, resulting in strong adsorption of CO on Rh/Al_2O_3 than on Rh/C. The CO species adsorbed on Rh/Al_2O_3 catalysts are stable according to the literature. Nehasil et al. reported a heat of CO adsorption of 120 kJ mol^{-1} in the limit of zero coverage,

which decreased with an increase in coverage θ, being 110 kJ mol^{-1} at θ = 1 [50]. Dulaurent et al. showed that the heat of CO adsorption depended on the type of CO species adsorbed on an Rh/Al_2O_3 catalyst [51]. It was reported to be 195 kJ mol^{-1} at θ = 0 and 103 kJ mol^{-1} at θ = 1 for the linear CO while 125 kJ mol^{-1} at θ = 0 and 75 kJ mol^{-1} at θ = 1 for the bridged CO. The heat of CO adsorption is larger for the linear CO than for the bridged CO. Dubois and Somorjai indicated that the bridged CO species on Rh(111) were removed by evacuation at 360 K while the coverage of the linear CO species was only slightly changed [52]. Using temperature programmed desorption (TPD), Belton et al. distinguished two different types of CO adsorbed on Rh(111) and determined the activation energy for desorption, which was 141 kJ mol^{-1} for one type (assigned to linear CO) and 125 kJ mol^{-1} for the other (bridged CO) [53]. These results obtained under dynamic methods (evacuation at a constant temperature and TPD) indicate that the linear CO species on Rh are more stable compared to the bridged ones. This is not in accordance with the present results that the linear CO species disappear on depressurization while the bridged CO species still remain. In our experiments, however, the catalyst was always exposed to the mixture of CO_2 and H_2 at decreasing pressures on the depressurization to ambient pressure at a constant temperature. This continuous exposure to the $CO_2 + H_2$ mixture is assumed to be important for the present results of the depressurization. The coverage of CO might be relatively large under the depressurization conditions used and so the bridged CO species should remain. Delouise et al. reported that, on Rh(111), the linear CO species were formed first at low coverage, followed by progressive appearance of the bridged ones with an increase in coverage [54].

Figure 17

It is reported by Chatterjee et al. that phenol is hydrogenated to cyclohexanone with a high selectivity > 97% with Pd/Al-MCM-41 catalyst at H_2 and CO_2 pressures of 4 MPa and 12 MPa, respectively [24]. The selectivity to cyclohexanone was found to depend on CO_2 pressure and it was < 60% at 7 MPa or below. Their similar Rh/Al-MCM-41 catalyst is less selective to the formation of cyclohexanone even at high CO_2 pressures. The difference between Pd and Rh on the same support would be ascribed to difference in their intrinsic natures. Unfortunately, these authors did not mention the possibility and significance of the formation of adsorbed CO in their catalytic hydrogenation reactions in dense phase CO_2 with Pd and Rh on Al-MCM-41. Recently, Liu et al. revealed the synergistic effect of supported Pd particles and solid Lewis acid sites for the selective hydrogenation of phenol to cyclohexanone [25]. The acid sites interact with C=O of cyclohexanone, preventing its further hydrogenation to the undesired cyclohexanol [25]. The Lewis acidity of the MCM-41 supports of Chatterjee's catalysts [24] may contribute to their high selectivity to cyclohexanone observed.

5. Conclusions

The following conclusions on the effects of CO_2 pressurization in hydrogenation of phenol with supported Rh catalysts may be withdrawn from the present results. The presence of compressed CO_2 retards the total rate of hydrogenation of phenol with Rh/C and Rh/Al_2O_3. This is crucial for the latter catalyst, for which its activity is completely lost in an early stage of reaction. For Rh/C, the selectivity to cyclohexanone in the presence of CO_2 does not depend on CO_2 pressure and is larger at high conversion levels > 70% than that obtained with CO_2. Molecular interactions of CO_2 are assumed to exist for cyclohexanone but not for phenol. The reactivity of carbonyl bond of cyclohexanone is suggested to increase by CO_2 but this is insignificant in determining the rate of hydrogenation of cyclohexanone to cyclohexanol. Possible reaction mechanisms involve direct transformations of phenol to either cyclohexanone and cyclohexanol and hydrogenation of cyclohexanone to cyclohexanol. It is suggested that the presence of CO_2 does not affect the direct transformations of phenol to either cyclohexanone or cyclohexanol but does retard the hydrogenation of cyclohexanone to cyclohexanol, resulting in the improved selectivity to cyclohexanone. It is confirmed that, during the hydrogenation reactions with Rh/C and Rh/Al_2O_3, CO is formed and adsorbed on the surface of these catalysts. This is one of important factors responsible for the retardation of the hydrogenation rate in the presence of CO_2. This CO adsorption is crucial for Rh/Al_2O_3; namely, the adsorption of CO on this catalyst is strong and so this causes the complete loss of its activity. The influence of CO_2 pressurization on the rates of hydrogenation of either phenol or cyclohexanone could be explained by several factors including volume expansion of liquid substrate phase, phase transition from gas-liquid-solid to gas-solid, and dilution of reacting species in either the liquid phase or the gas phase.

Acknowledgement

This work was supported in part by the Japan Society for the Promotion of Science (JSPS) with Grant-in-Aid for Scientific Research (B) 18360378 and also by JSPS and CAS (Chinese Academy of Sciences) under the Japan - China Research Cooperative Program. The authors are thankful to Ms. M. Furuyuki, Mr. M. Hasegawa, and Dr. T. Akashi of Hokkaido University for their help in reaction, phase behavior, and XPS measurements.

References

[1] I. Doddgson, K. Friffin, G. Barberis, F. Pignataro, G. Tauszik, A low cost phenol to cyclohexanone process, Chem. Ind., 18 (1989) 830-833.

[2] G. Neri, A.M. Visco, A. Donato, C. Milone, M. Malentacchi, G. Gubitosa, Hydrogenation of phenol to cyclohexanone over palladium and alkali-doped palladium catalysts, Appl. Catal. A: Gen., 110 (1994) 49-59.

[3] S. Narayanan, K. Krishna, Hydrotalcite-supported palladium catalysts. Part I: Preparation, characterization of hydrotalcites and palladium on uncalcined hydrotalcites for CO chemisorption and phenol hydrogenation, Appl. Catal. A: Gen., 174 (1998) 221-229.

[4] Y. Z. Chen, C. W. Liaw, I. Lee, Selective hydrogenation of phenol to cyclohexanone over palladium supported on calcined Mg/Al hydrotalcite, Appl. Catal. A: Gen., 177 (1999) 1-8.

[5] N. Mahata, V. Vishwanathan, Gas phase hydrogenation of phenol over supported palladium catalysts, Catal. Today, 49 (1999) 65-69.

[6] P. Claus, H. Berndt, C. Mohr, J. Radnik, E. Shin, M. A. Keane, Pd/MgO: catalyst characterization and phenol hydrogenation activity, J. Catal., 192 (2000) 88-97.

[7] N. Mahata, V. Vishwanathan, Influence of palladium precursors on structural properties and phenol hydrogenation characteristics of supported palladium catalysts, J. Catal., 196 (2000) 262-270.

[8] S. Narayanan, K. Krishna, Hydrotalcite-supported palladium catalysts. Part II. Preparation, characterization of hydrotalcites and palladium hydrotalcites for CO chemisorption and phenol hydrogenation, Appl. Catal. A: Gen., 198 (2000) 13-21.

[9] N. Mahata, K.V. Raghavan, V. Vishwanathan, C. Park, M. A. Keane, Phenol hydrogenation over palladium supported on magnesia: relationship between catalyst structure and performance, Phys. Chem. Chem. Phys., 3 (2001) 2712-2719.

[10] S. Scire, S. Minico, C. Crisafulli, Selective hydrogenation of phenol to cyclohexanone over supported Pd and Pd-Ca catalysts: an investigation on the influence of different supports and Pd precursors, Appl. Catal. A: Gen., 235 (2002) 21-31.

[11] S. G. Shore, E. Ding, C. Park, M. A. Keane, Vapor phase hydrogenation of phenol over silica supported Pd and Pd-Yb catalysts, Catal. Commun., 3 (2002) 77-84.

[12] K. V. R. Chary, D. Naresh, V. Vishwanathan, M. Sadakane, W. Ueda, Vapour phase hydrogenation of phenol over Pd/C catalysts: a relationship between dispersion, metal area and hydrogenation activity, Catal. Commun., 8 (2007) 471-477.

[13] J. R. Gonzalez-Velasco, M. P. Gonzalez-Marcos, S. Arnaiz, J. I. Gutierrez-Ortiz, M. A. Gutierrez-Ortiz, Activity and selectivity of palladium catalysts during the liquid-phase hydrogenation of phenol. influence of temperature and pressure, Ind. Eng. Chem. Res., 34 (1995) 1031-1036.

[14] L. Zhuang, H. Li, M. Qiao, Liquid phase hydrogenation of phenol to cyclohexenone over a Pd–La–B amorphous catalyst, Chem. Lett., 3 (2003) 1072-1073.

[15] P. Makowski, R. D. Caken, M. Antonietti, F. Goettmann, M.-M. Titirici, Selective partial hydrogenation of hydroxy aromatic derivatives with palladium nanoparticles supported on hydrophilic carbon, Chem. Commun., (2008) 999-1001.

[16] H. Li, J. Liu, H. Li, Liquid-phase selective hydrogenation of phenol to cyclohexanone over

the Ce-doped Pd–B amorphous alloy catalyst, Mater. Lett., 62 (2008) 297-300.
[17] A. Baiker, Supercritical fluids in heterogeneous catalysis, Chem. Rev., 99 (1999) 453-474.
[18] P. G. Jessop, T. Ikariya, R. Noyori, Homogeneous catalysis in supercritical fluids, Chem. Rev., 99 (1999) 475-494.
[19] B. M. Bhanage, S. Fujita, M. Arai, Heck reactions with various types of palladium complex catalysts: application of multiphase catalysis and supercritical carbon dioxide, J. Organometal. Chem., 687 (2003) 211-218.
[20] C. M. Rayner, The potential of carbon dioxide in synthetic organic chemistry, Org. Proc. Res. Dev., 11 (2007) 121-132.
[21] A. Kruse, H. Vogel, Heterogeneous catalysis in supercritical media: 1. carbon dioxide, Chem. Eng. Technol., 31 (2008) 23-32.
[22] C. Rode, U. Joshi, O. Sato, M. Shirai, Catalytic ring hydrogenation of phenol under supercritical carbon dioxide, Chem. Commun., (2003) 1960-1961.
[23] H. Wang, F. Zhao, S. Fujita, M. Arai, Hydrogenation of phenol in $scCO_2$ over carbon nanofiber supported Rh catalyst, Catal. Commun., 9 (2008) 362-368.
[24] M. Chatterjee, K. Kawanami, M, Sato, A. Chatterjee, T. Yokoyama, T. Suzuki, Hydrogenation of phenol in supercritical carbon dioxide catalyzed by palladium supported on Al-MCM-41: a facile route for one-pot cyclohexanone formation, Adv. Synth. Catal., 351 (2009) 1912-1924.
[25] H. Liu, T. Jiang, B. Han, S. Liang, Y. Zhou, Selective phenol hydrogenation to cyclohexanone over a dual supported Pd-Lewis acid catalyst, Science, 326 (2009) 1250-1252.
[26] M. Arai, S. Fujita, M. Shirai, Multiphase catalytic reactions in/under dense phase CO_2, J. Supercrit. Fluids, 47 (2009) 351-356.
[27] F. Zhao, S. Fujita, J. Sun, Y. Ikushima, M. Arai, Carbon dioxide-expanded liquid substrate phase: an effective medium for selective hydrogenation of cinnamaldehyde to cinnamyl alcohol, Chem. Commun., (2004) 2326-2327.
[28] F. Zhao, S. Fujita, S. Akihara, M. Arai, Hydrogenation of benzaldehyde and cinnamaldehyde in compressed CO_2 medium with a Pt/C catalyst: a study on molecular interactions and pressure effects, J. Phys. Chem. A, 109 (2005) 4419-4424.
[29] R. Liu, F. Zhao, S. Fujita, M. Arai, Selective hydrogenation of citral with transition metal complexes in supercritical carbon dioxide, Appl. Catal. A: Gen., 316 (2007) 127-133.
[30] S. Fujita, T. Tanaka, Y. Akiyama, K. Asai, J. Hao, F. Zhao, M. Arai, Impact of carbon dioxide pressurization on liquid phase organic reactions: a case study on Heck and Diels-Alder reactions, Adv. Synth. Catal., 350 (2008) 1615-1625.
[31] Y. Akiyama, S. Fujita, H. Senboku, C.M. Rayner, S.A. Brough, M. Arai, An in situ high pressure FTIR study on molecular interactions of ketones, esters, and amides with dense phase carbon dioxide J. Supercrit. Fluids, 46 (2008) 197-205.
[32] G. Musie, M. Wei, B. Subramaniam, D. H. Busch, Catalytic oxidations in carbon

dioxide-based reaction media, including novel CO_2-expanded phases, Coord. Chem. Rev., 219-221 (2001) 789-820.

[33] B. Subramaniam, C. J. Lyon, V. Arunajatesan, Environmentally benign multiphase catalysis with dense phase carbon dioxide, Appl. Catal. B Environ., 37 (20029 279-292.

[34] B. Kerler, R. E. Robinson, A. S. Borovik, B. Subramaniam, Application of CO_2-expanded solvents in heterogeneous catalysis: a case study, Appl. Catal. B Environ., 49 (2004) 91-98.

[35] P.G. Jessop, B. Subramaniam, Gas-expanded liquids, Chem. Rev., 107 (2007) 2666-2694.

[36] G. R. Akien, M. Poliakoff, A critical look at reactions in class I and II gas-expanded liquids using CO_2 and other gases, Green Chem., 11 (2009) 1083-1100.

[37] D. Ferri, T. Bürgi, A. Baiker, Probing boundary sites on a Pt/Al_2O_3 model catalyst by CO_2 hydrogenation and in situ ATR-IR spectroscopy of catalytic solid–liquid interfaces, Phys. Chem. Chem. Phys., 4 (2002) 2667-2672.

[38] B. Minder, T. Mallat, K.H. Pickel, K. Steiner, A. Baiker, Enantioselective hydrogenation of ethyl pyruvate in supercritical fluids, Catal. Lett., 1 (1995) 1-9.

[39] S. Ichikawa, M. Tada, Y. Iwasawa, T. Ikariya, The role of carbon dioxide in chemoselective hydrogenation of halonitroaromatics over supported noble metal catalysts in supercritical carbon dioxide, Chem. Commun., (2005) 924-926.

[40] M. Burgener, D. Ferri, J.-D- Grunwaldt, T. Mallat, A. Baiker, Supercritical carbon dioxide: an inert solvent for catalytic hydrogenation?, J. Phys. Chem. B, 109 (2005) 16794-16800.

[41] V. Arunajatesan, B. Subramaniam, K. W. Hutchenson, F. E. Herkes, In situ FTIR investigations of reversewater gas shift reaction activity at supercritical conditions, Chem. Eng. Sci., 62 (2007) 5062-5069.

[42] C. D. Zeinalipour-Yazdi, A. L. Cooksy, A. M. Efstathiou, A diffuse reflectance infrared Fourier-transform spectra and density functional theory study of CO adsorption on $Rh/\gamma\text{-}Al_2O_3$, J. Phys. Chem. C, 111 (2007) 13872-13878.

[43] J. Ryczkowski, IR spectroscopy in catalysis, Catal. Today, 68 (2001) 263-381.

[44] G. A. Somorjai, Introduction to Surface Chemistry and Catalysis, Wiley, 1994, p. 328.

[45] G. Busca, J. Lamotte, J.-C. Lavalley, V. Lorenzelli, FT-IR study of the adsorption and transformation of formaldehyde on oxide surfaces, J. Am. Chem. Soc., 109 (1987) 5197-5202.

[46] A. Erdöhelyi, M. Pásztor, F. Solymosi, Catalytic hydrogenation of CO_2 over supported palladium, J. Catal., 98 (1986) 166-177.

[47] J. J. Benitez, R. Alvero, I. Carrizosa, J. A. Odriozola, In situ DRIFTS study of adsorbed species in the hydrogenation of carbon oxides, Catal. Today, 9 (1991) 53-60.

[48] S. Fujita, N. Takezawa, Difference in the selectivity of CO and CO_2 methanation reactions, Chem. Eng. J., 68 (1997) 63-68.

[49] K. Nakanishi, P. H. Solomon, Infrared Absorption Spectroscopy, 2nd Ed., Holden-Day, 1977, pp. 38-44.

[50] V. Nehasil, I. Stara, V. Matolin, Study of CO desorption and dissociation on Rh surfaces,

Surf. Sci., 331 (1995) 105-109.

[51] O. Dulaurent, K. Chandes, C. Bouly, D. Bianchi, Heat of adsorption of carbon monoxide on a Pd/Rh three-way catalyst and on a Rh/Al_20_3 solid, J. Catal., 192 (2000) 262-272.

[52] L. H. Dubois, G. A. Somorjai, The chemisorption of CO and CO_2 on Rh(111) studied by high resolution electron energy loss spectroscopy, Surf. Sci., 91 (1980) 514-532.

[53] D. N. Belton, S. J. Schmieg, Effect of Rh particle size on CO desorption from Rh/alumina model catalysts, Surf. Sci., 202 (1988) 238-254.

[54] L. A. Delouise, E. J. White, N. Winograd, Characterization of CO binding sites on Rh(111) and Rb(331) surfaces by XPS and LEED: comparison to EELS results, Surf. Sci., 147 (1984) 252-262.

Captions of Table, Figures and Scheme

Table 1 Adsorption bands observed and possible assignments

Table 2 Rate constants used in the simulation of reaction kinetics

Table 3 Comparison of the activity and the selectivity between Rh/C and Rh/Al_2O_3 for phenol hydrogenation in the absence of CO_2.

Fig. 1. Variations of phenol conversion (□) and yields of cyclohexanone (●) and cyclohexanol (○) with time over Rh/C (a) in the absence of CO_2 and (b) in the presence of 16 MPa CO_2. Reaction conditions: Rh/C, 10 mg for (a) and 20 mg for (b); phenol, 10.6 mmol; H_2, 4 MPa; temperature, 323 K.

Fig. 2. Influence of CO_2 on the relationship between selectivity to cyclohexanone and phenol conversion over Rh/C. CO_2 pressure = 0 (●), 4 (▲), 8 (■), 11 (○), 14 (◊) and 16 MPa (□).

Fig. 3. Influence of CO_2 pressure on the initial rate of hydrogenation of (a) phenol and (b) cyclohexanone over Rh/C. Reaction conditions: Rh/C, 2.5 mg; phenol, 10.6 mmol; H_2, 4 MPa; temperature, 323 K; time, 5 min for phenol and 10 min for cyclohexanone.

Fig. 4. Variations of phenol conversion (□) and yields of cyclohexanone (●) and cyclohexanol (○) with time over Rh/Al_2O_3 in the absence of CO_2. Reaction conditions: Rh/Al_2O_3, 10 mg; phenol, 10.6 mmol; H_2, 4 MPa; temperature, 323 K.

Fig. 5. Variations of phenol conversion (□) and yields of cyclohexanone (●) and cyclohexanol (○) with time over Rh/Al_2O_3 in the presence of CO_2 at (a) 14 MPa and (b) 8 MPa. Reaction conditions: Rh/Al_2O_3, 50 mg; phenol, 10.6 mmol; H_2, 4 MPa; temperature, 323 K.

Fig. 6. Influence of CO_2 on the relationship between selectivity to cyclohexanone and phenol conversion over Rh/Al_2O_3. CO_2 pressure = 0 (●), 4 (▲), 8 (■) and 14 (◊) MPa.

Fig. 7. Solubility of phenol (□), cyclohexanone (●) and cyclohexanol (○) into $scCO_2$ in the presence of 4 MPa H_2 at 323 K.

Fig. 8. Photographs of (a) phenol and (b) cyclohexanone liquid phases taken under various pressures of CO_2 at 323 K in the presence of 4 MPa H_2.

Fig. 9. Variation of the volume of cyclohexanone with CO_2 pressure at 323 K in the presence of 4

MPa H_2.

Fig. 10. FT-IR spectra of cyclohexanone. (a), liquid; (b), gas; (c) in 4 MPa CO_2; (d), in 8 MPa CO_2; (e), in16 MPa CO_2. Spectra c, d and e were measured in the presence of 4 MPa H_2.

Fig. 11. *In situ* high-pressure FTIR spectra collected at 50°C for Rh/Al_2O_3 sample in the presence of 4 MPa H_2 and 4 MPa CO_2 (a-d) or 16 MPa CO_2 (e-h). The spectra were collected shortly after introduction of CO_2 (a, e) and after different times of 1 h (b, f), 2 h (c, g) and 4 h (d, h).

Fig. 12. *In situ* high-pressure FTIR spectra collected at 50°C for Rh/C sample in the presence of 4 MPa H_2 and 4 MPa CO_2 (a-d) or 16 MPa CO_2 (e-h). The spectra were collected shortly after introduction of CO_2 (a, e) and after different times of 1 h (b, f), 2 h (c, g) and 4 h (d, h).

Fig. 13. *In situ* high-pressure FTIR spectra collected at 50°C for Rh/Al_2O_3 (a-c) and Rh/C (d-f) samples in the presence of 4 MPa H_2 and 16 MPa CO_2 (a, d), after depressurization (b, e) and after purging with H_2 (c, f).

Fig. 14. Variations of phenol conversion (□) and yields of cyclohexanone (●) and cyclohexanol (○) with time over Rh/C (a) in the absence of CO_2 and in the presence of CO_2 at 4 MPa (b) and (c) 16 MPa. Solid lines were determined by simulation for which k_2, k_3, and k_4 values listed in Table 2 were used. Reaction conditions were the same as those for Fig. 1.

Fig. 15. Variations of phenol conversion (□) and yields of cyclohexanone (●) and cyclohexanol (○) with time over Rh/Al_2O_3 in the absence of CO_2. Solid lines were determined by simulation for which k_2, k_3, and k_4 values listed in Table 2 were used. Reaction conditions were the same as those for Fig. 4.

Fig. 16. Influence of CO_2 on the relationship between selectivity to cyclohexanone and phenol conversion over (a) Rh/C and (b) Rh/Al_2O_3. Circles and squares represent experimental values observed in the absence and the presence of 16MPa CO_2, respectively. Solid and broken lines were obtained by simulation with the rate constants listed in Table 2.

Fig. 17. XPS spectra of (a) Rh/C and (b) Rh/Al_2O_3.

Scheme 1. Reaction pathways of phenol hydrogenation.

Figures, Tables, and Scheme in the order of appearance

Fig. 1

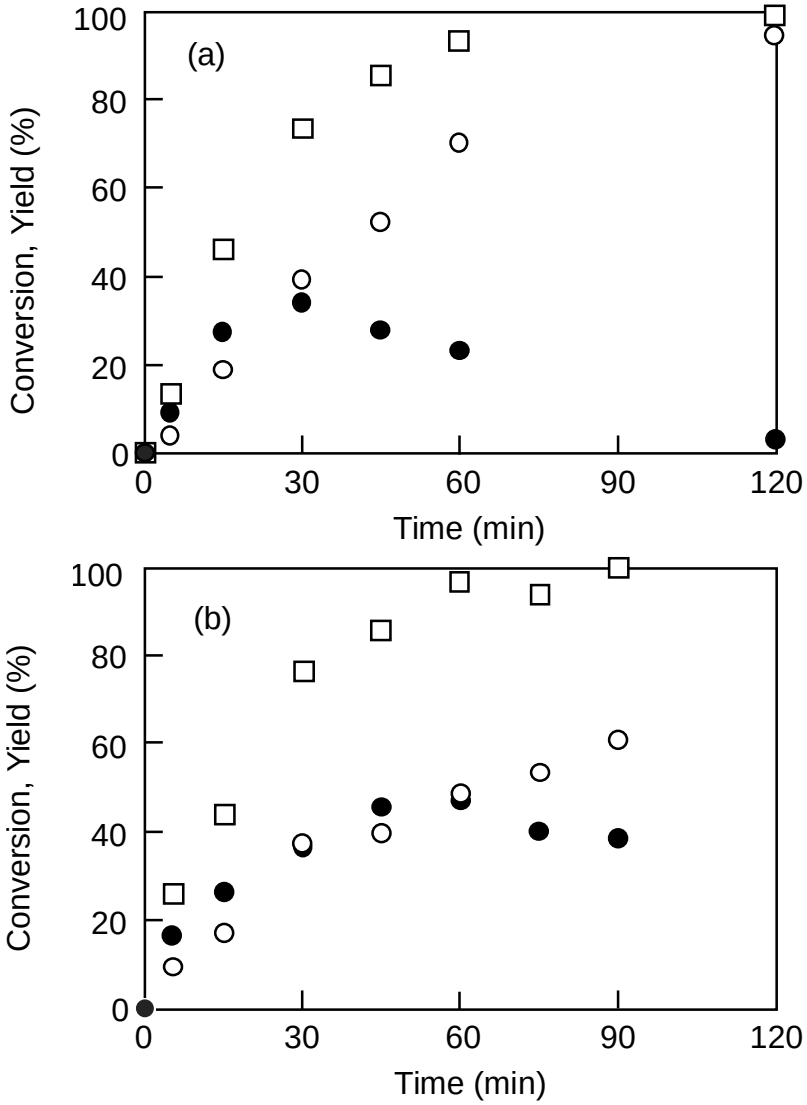

Fig. 1. Variations of phenol conversion (□) and yields of cyclohexanone (●) and cyclohexanol (○) with time over Rh/C (a) in the absence of CO_2 and (b) in the presence of 16 MPa CO_2. Reaction conditions: Rh/C, 10 mg for (a) and 20 mg for (b); phenol, 10.6 mmol; H_2, 4 MPa; temperature, 323 K.

Fig. 2

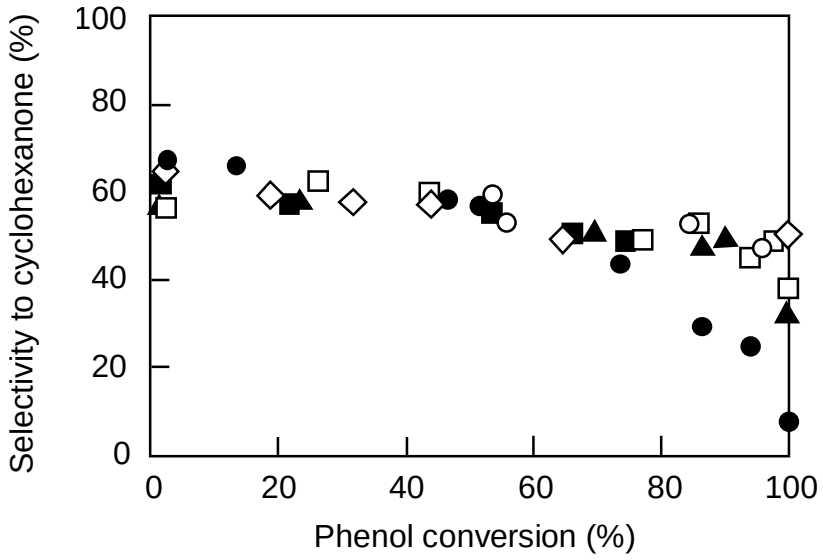

Fig. 2. Influence of CO_2 on the relationship between selectivity to cyclohexanone and phenol conversion over Rh/C. CO_2 pressure = 0 (●), 4 (▲), 8 (■), 11 (○), 14 (◊) and 16 MPa (□).

Fig. 3

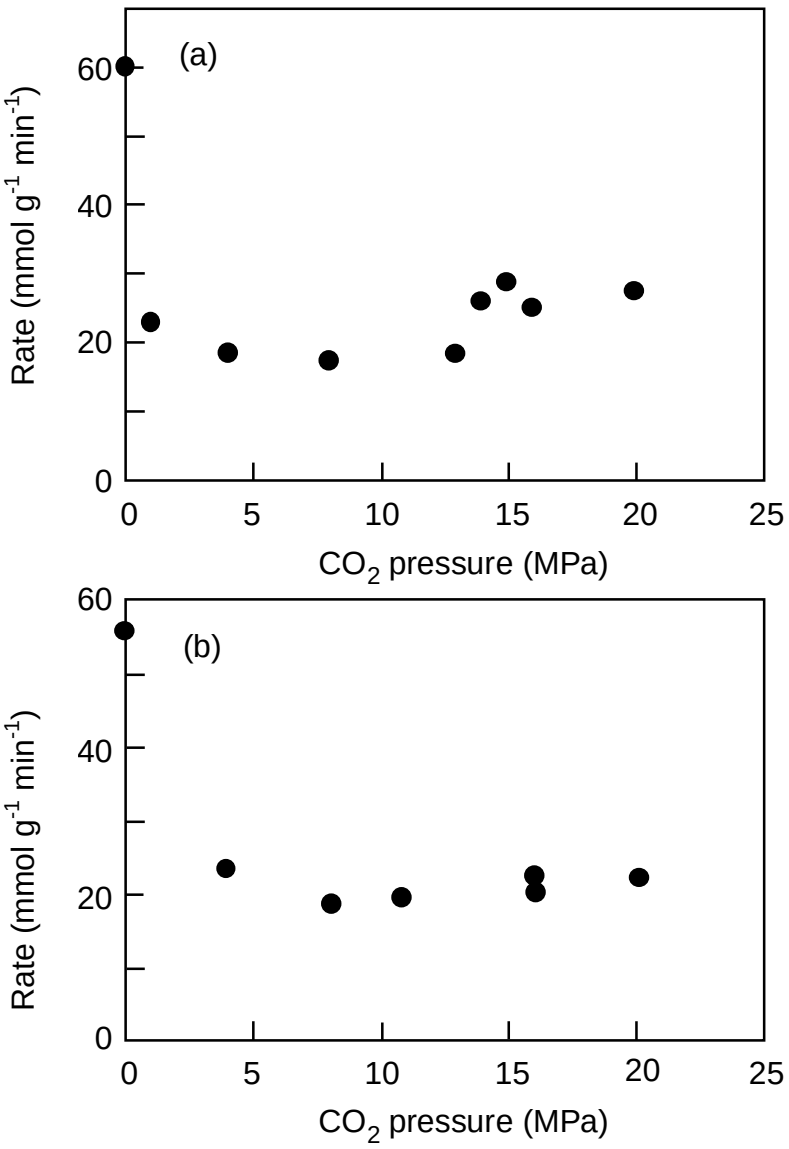

Fig. 3. Influence of CO_2 pressure on the initial rate of hydrogenation of (a) phenol and (b) cyclohexanone over Rh/C. Reaction conditions: Rh/C, 2.5 mg; phenol, 10.6 mmol; H_2, 4 MPa; temperature, 323 K; time, 5 min for phenol and 10 min for cyclohexanone.

Fig. 4

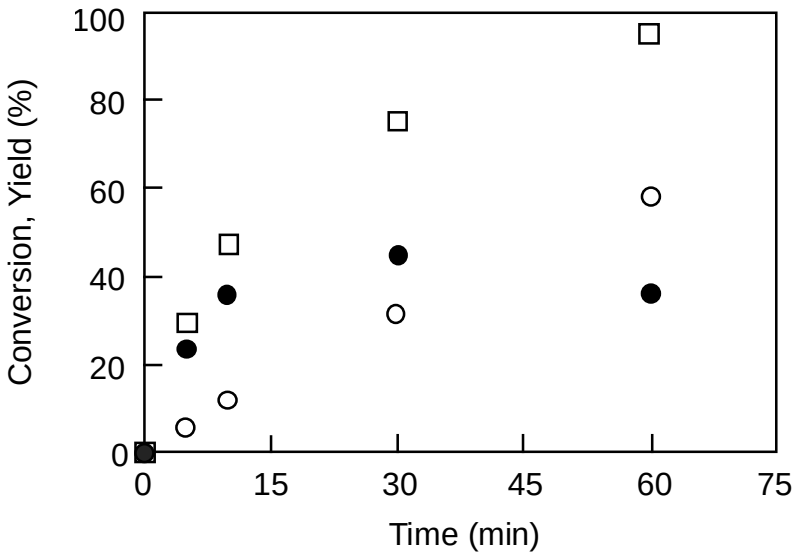

Fig. 4. Variations of phenol conversion (□) and yields of cyclohexanone (●) and cyclohexanol (○) with time over Rh/Al_2O_3 in the absence of CO_2. Reaction conditions: Rh/Al_2O_3, 10 mg; phenol, 10.6 mmol; H_2, 4 MPa; temperature, 323 K.

Fig. 5

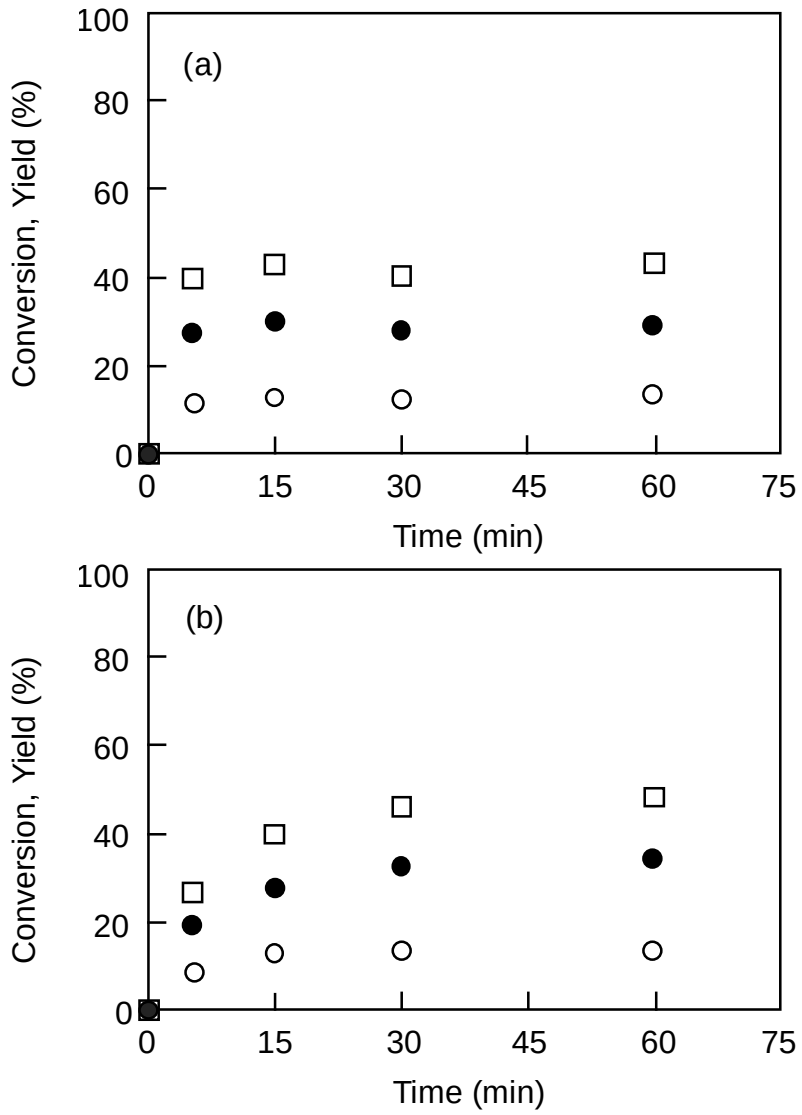

Fig. 5. Variations of phenol conversion (□) and yields of cyclohexanone (●) and cyclohexanol (○) with time over Rh/Al_2O_3 in the presence of CO_2 at (a) 14 MPa and (b) 8 MPa. Reaction conditions: Rh/Al_2O_3, 50 mg; phenol, 10.6 mmol; H_2, 4 MPa; temperature, 323 K.

Fig. 6

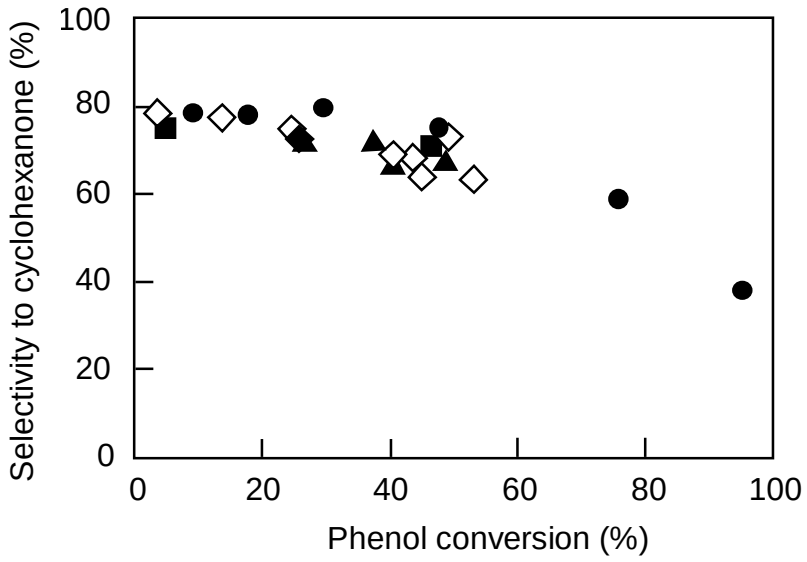

Fig. 6. Influence of CO_2 on the relationship between selectivity to cyclohexanone and phenol conversion over Rh/Al_2O_3. CO_2 pressure = 0 (●), 4 (▲), 8 (■) and 14 (◊) MPa.

Fig. 7

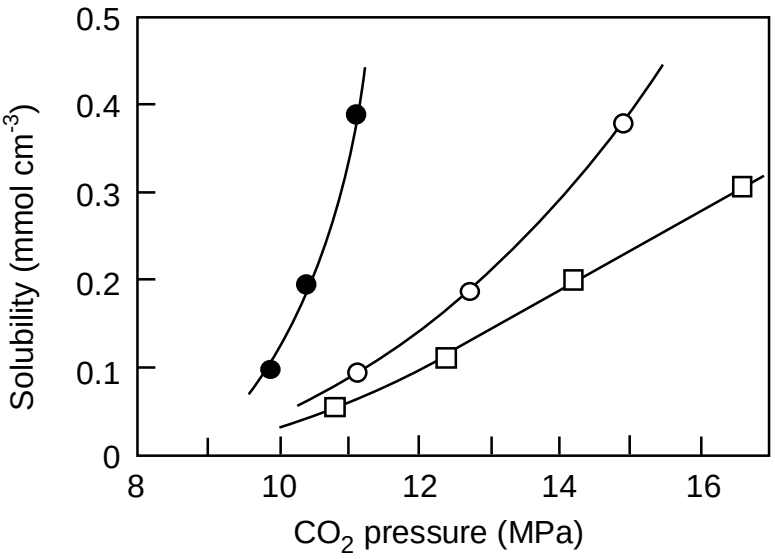

Fig. 7. Solubility of phenol (□), cyclohexanone (●) and cyclohexanol (○) into $scCO_2$ in the presence of 4 MPa H_2 at 323 K.

Fig. 8

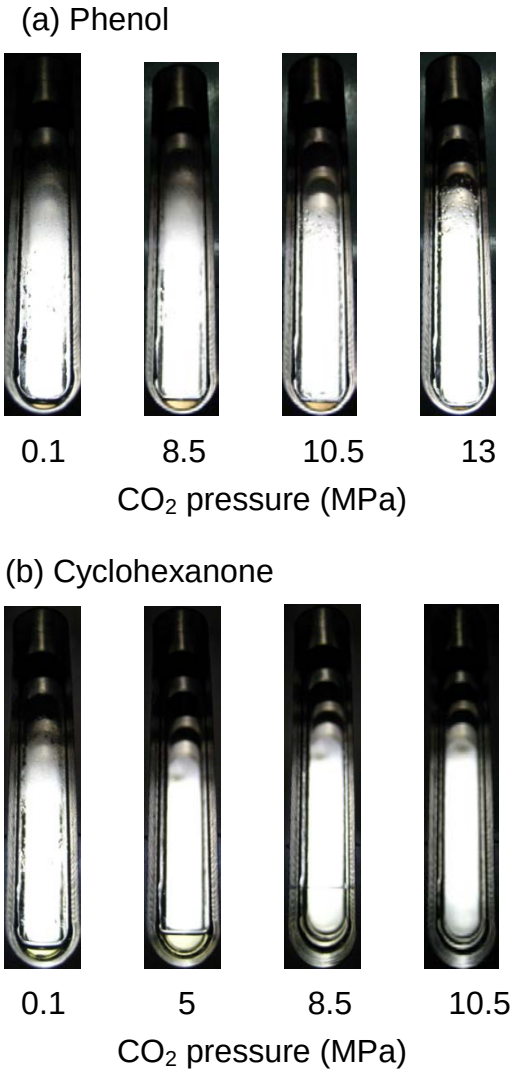

Fig. 8. Photographs of (a) phenol and (b) cyclohexanone liquid phases taken under various pressures of CO_2 at 323 K in the presence of 4 MPa H_2.

Fig. 9

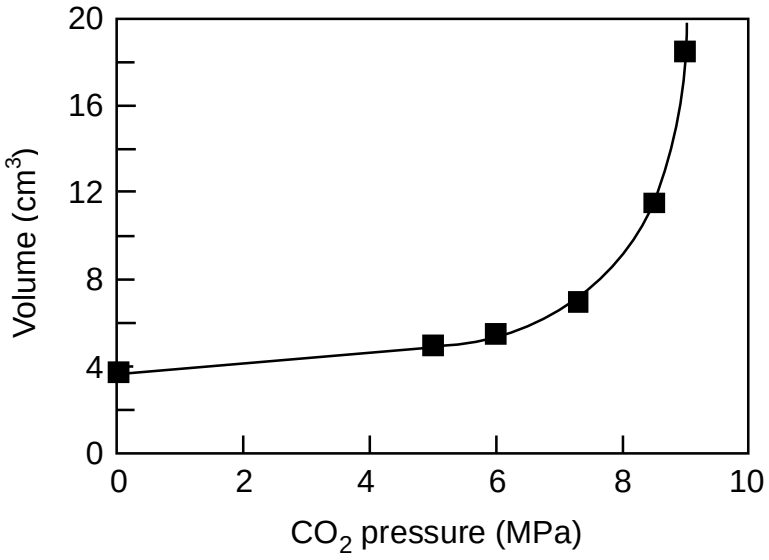

Fig. 9. Variation of the volume of cyclohexanone with CO_2 pressure at 323 K in the presence of 4 MPa H_2.

Fig. 10

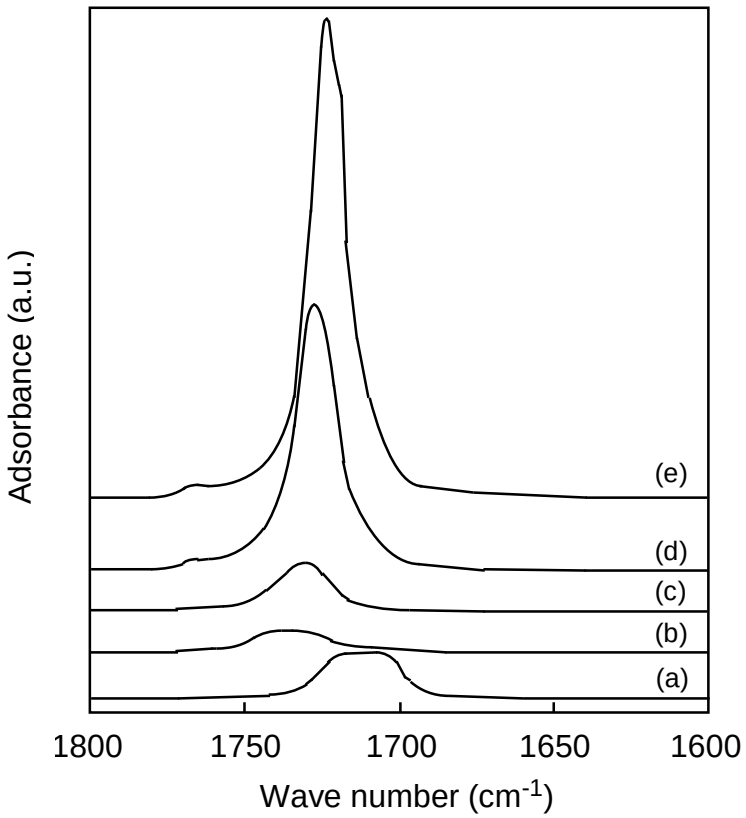

Fig. 10. FT-IR spectra of cyclohexanone. (a), liquid; (b), gas; (c) in 4 MPa CO_2; (d), in 8 MPa CO_2; (e), in16 MPa CO_2. Spectra c, d and e were measured in the presence of 4 MPa H_2.

Fig. 11

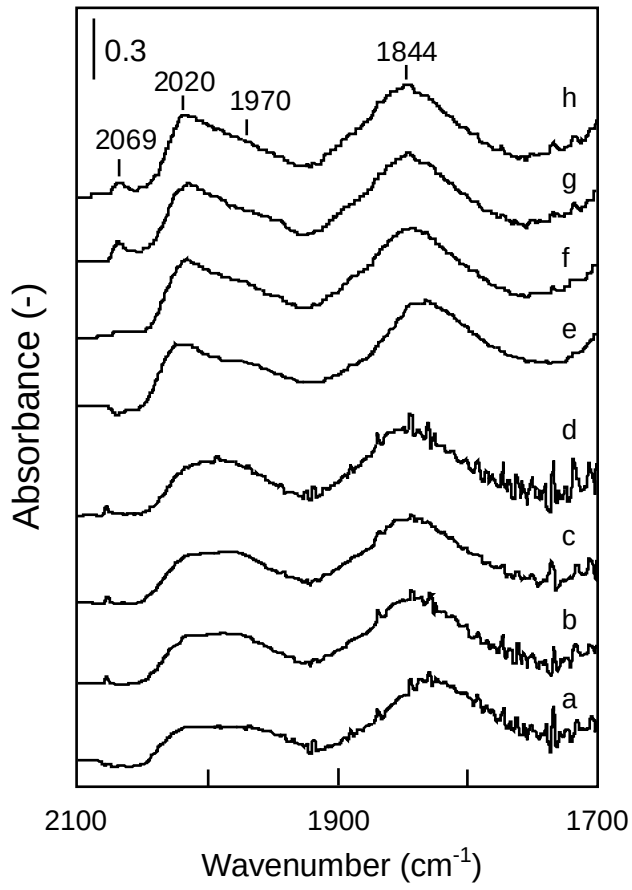

Fig. 11. *In situ* high-pressure FTIR spectra collected at 50°C for Rh/Al_2O_3 sample in the presence of 4 MPa H_2 and 4 MPa CO_2 (a-d) or 16 MPa CO_2 (e-h). The spectra were collected shortly after introduction of CO_2 (a, e) and after different times of 1 h (b, f), 2 h (c, g) and 4 h (d, h).

Table 1 Adsorption bands observed and possible assignments

Rh/Al_2O_3	Rh/C	Assignment [a]
2069 cm^{-1}, 2020 cm^{-1}	2069 cm^{-1}	Linear
1970 cm^{-1}	1945 cm^{-1}	Linear or Dicarbonyl
1844 cm^{-1}	—[b]	Bridged or Triply bridged
1600 cm^{-1} — 1200 cm^{-1}		Formate (and/or -COOH, -COO-) [c]

a. Ref. 42-45, 49.

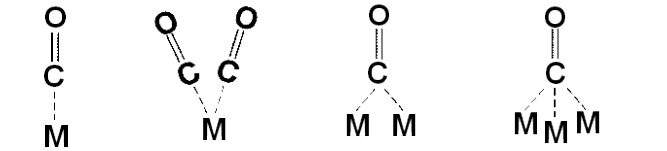

Linear Dicarbonyl Bridged Triply bridged

b. No corresponding absorption bands were observed

c. $\nu_a(CO)$ appears at a larger wavenumber compared with $\nu_s(CO)$.

Fig. 12

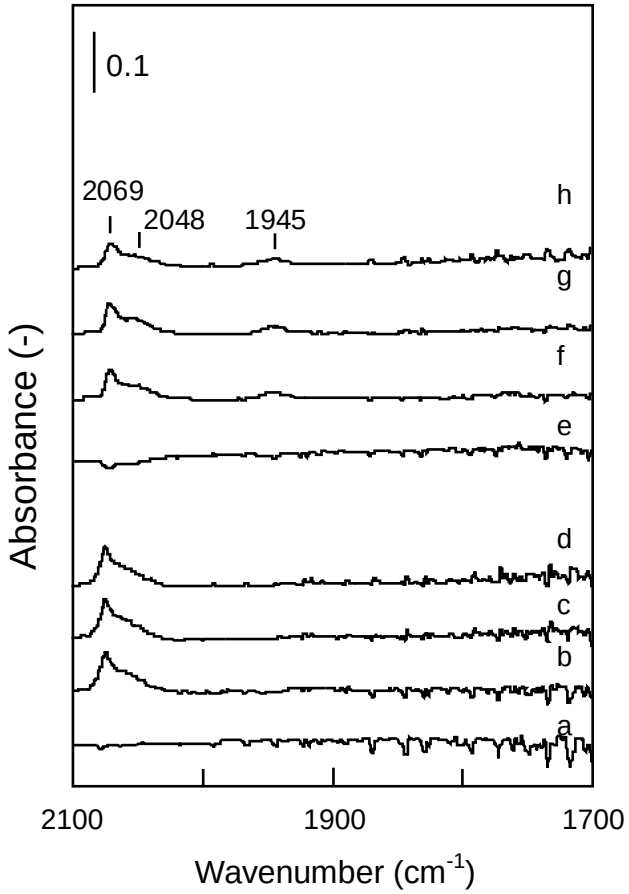

Fig. 12. *In situ* high-pressure FTIR spectra collected at 50°C for Rh/C sample in the presence of 4 MPa H_2 and 4 MPa CO_2 (a-d) or 16 MPa CO_2 (e-h). The spectra were collected shortly after introduction of CO_2 (a, e) and after different times of 1 h (b, f), 2 h (c, g) and 4 h (d, h).

Fig. 13

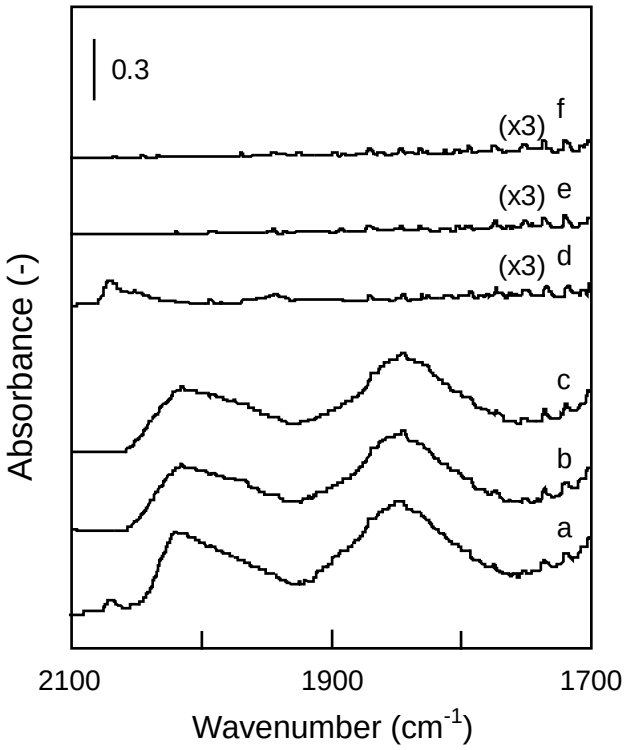

Fig. 13. *In situ* high-pressure FTIR spectra collected at 50°C for Rh/Al_2O_3 (a-c) and Rh/C (d-f) samples in the presence of 4 MPa H_2 and 16 MPa CO_2 (a, d), after depressurization (b, e) and after purging with H_2 (c, f).

Scheme 1

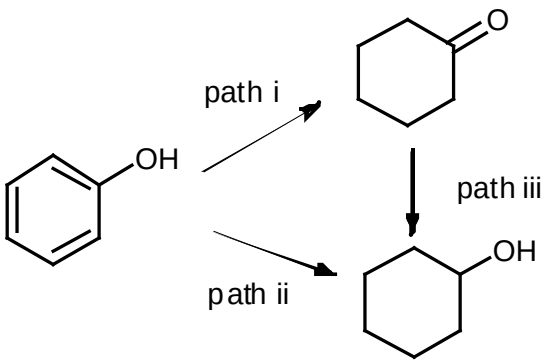

Scheme 1. Reaction pathways of phenol hydrogenation.

Fig. 14

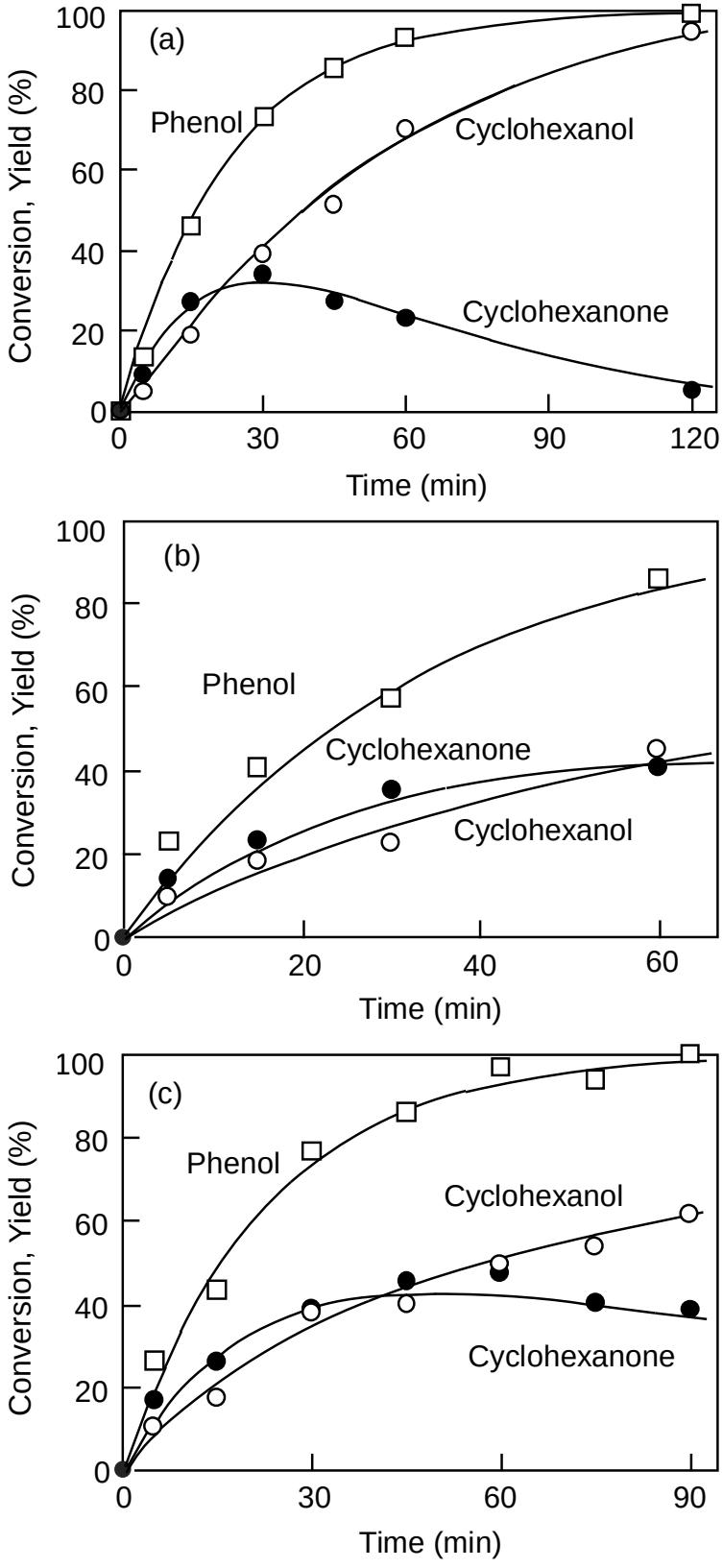

Fig. 14. Variations of phenol conversion (□) and yields of cyclohexanone (●) and cyclohexanol (○) with time over Rh/C (a) in the absence of CO_2 and in the presence of CO_2 at 4 MPa (b) and (c) 16 MPa. Solid lines were determined by simulation for which k_2, k_3, and k_4 values listed in Table 2 were used. Reaction conditions were the same as those for Fig. 1.

Table 2 Rate constants used in the simulation of reaction kinetics

Catalyst	P_{CO2} (MPa)	Phase [a]	C_0 [b] (mol/L)	Rate constant (min^{-1} g-cat^{-1})[c]		
				k_1	k_2	k_3
Rh/C	0	G-L-S	11.2	3.0	1.5	2.4
	4	G-L-S	11.2	0.9	0.6	0.2
	16	G-S	0.21	1.4	0.9	0.3
Rh/Al_2O_3	0	G-L-S	11.2	4.7	1.0	1.8

[a] Phases present in the reaction mixture: G, L, and S indicate gas (CO_2, H_2, and/or phenol), liquid substrate (phenol), and solid (catalyst) phases, respectively.

[b] Initial concentration of phenol: For G-L-S system, concentration in pure liquid phenol; For G-S system, concentration in the gas phase (in the whole reactor volume).

[c] at 323 K.

Fig. 15

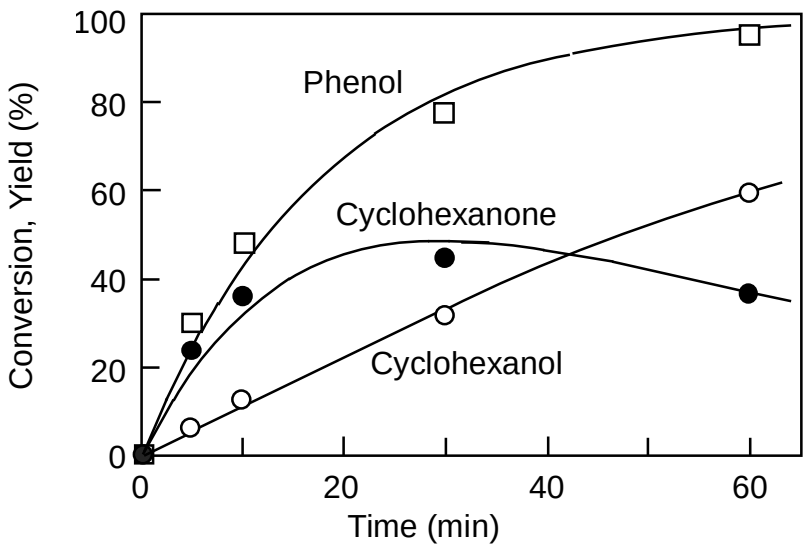

Fig. 15. Variations of phenol conversion (□) and yields of cyclohexanone (●) and cyclohexanol (○) with time over Rh/Al_2O_3 in the absence of CO_2. Solid lines were determined by simulation for which k_2, k_3, and k_4 values listed in Table 2 were used. Reaction conditions were the same as those for Fig. 4.

Fig. 16

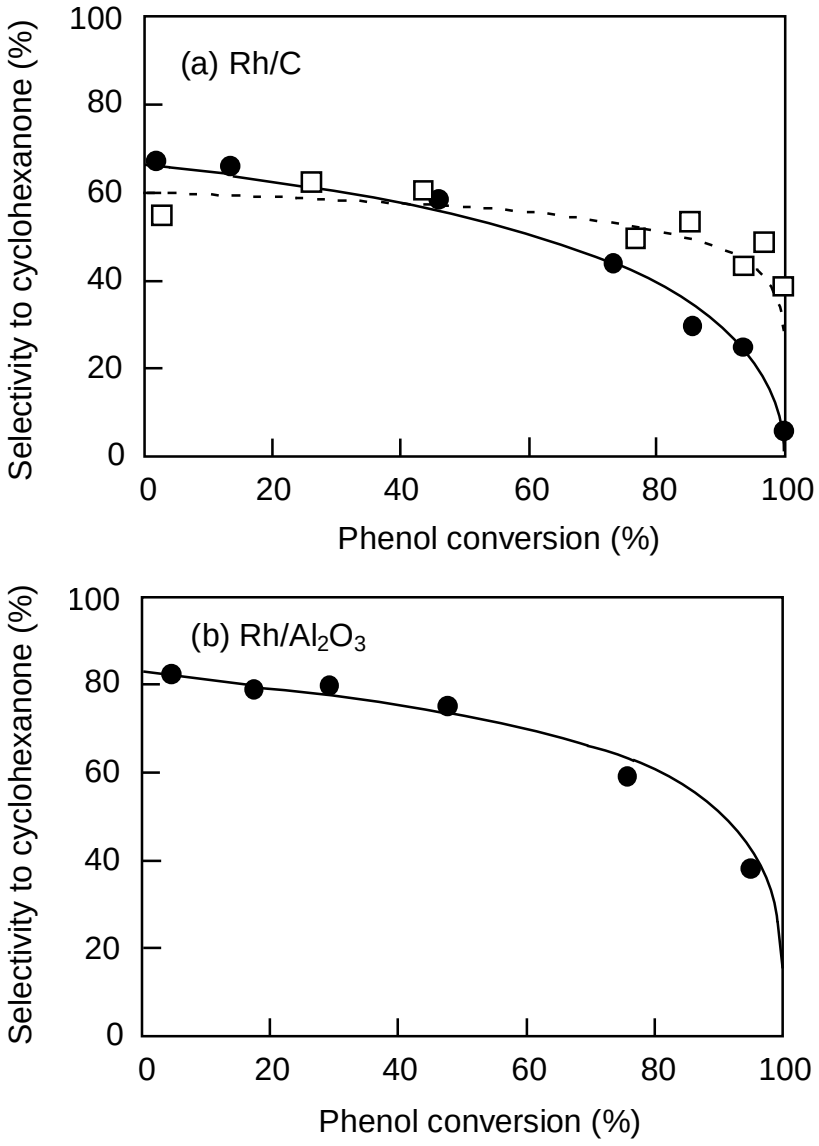

Fig. 16. Influence of CO_2 on the relationship between selectivity to cyclohexanone and phenol conversion over (a) Rh/C and (b) Rh/Al_2O_3. Circles and squares represent experimental values observed in the absence and the presence of 16MPa CO_2, respectively. Solid and broken lines were obtained by simulation with the rate constants listed in Table 2.

Table 3 Comparison of the activity and the selectivity between Rh/C and Rh/Al_2O_3 for phenol hydrogenation in the absence of CO_2.

Catalyst	Rh dispersion[a] (%)	Reaction rate[b] (mmol min^{-1} g-$cat.^{-1}$)	TOF[c] (s^{-1})	Selectivity to cyclohexanone (%)[d]	k_1/k_2[e] (-)
Rh/C	44.3	47.7	3.71	66.7	2.0
Rh/Al_2O_3	30.9	60.4	6.70	82.5	4.7

Reaction conditions: catalyst, 10 mg; phenol, 10.6 mmol; H_2, 4 MPa; temperature, 323 K; time 5 min.

[a] Determined by H_2 adsorption.

[b] Estimated from the rate constants listed in Table 1 and the initial amount of phenol.

[c] Turn-over frequency. Molecules of phenol consumed per an exposed Rh atom per unit time.

[d] Estimated from an equation of $k_1/(k_1 + k_2)$ and the rate constants listed in Table 1.

[e] Estimated from the rate constants listed in Table 1.

Fig. 17

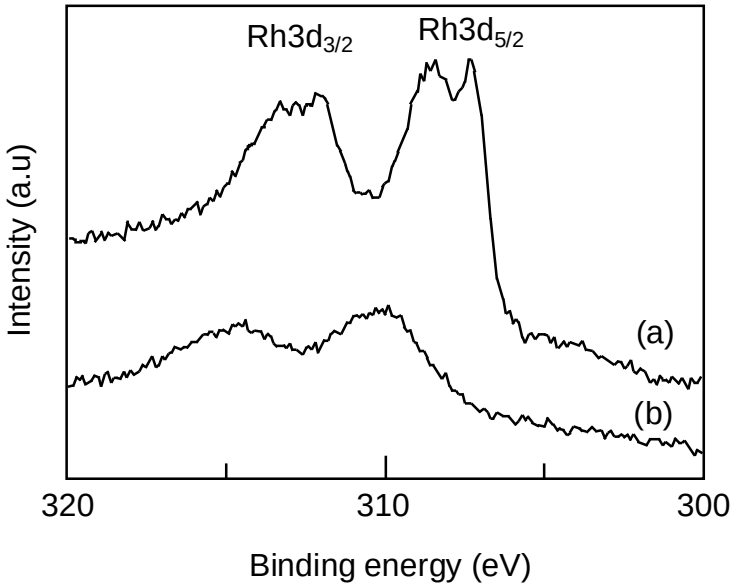

Fig. 17. XPS spectra of (a) Rh/C and (b) Rh/Al_2O_3.